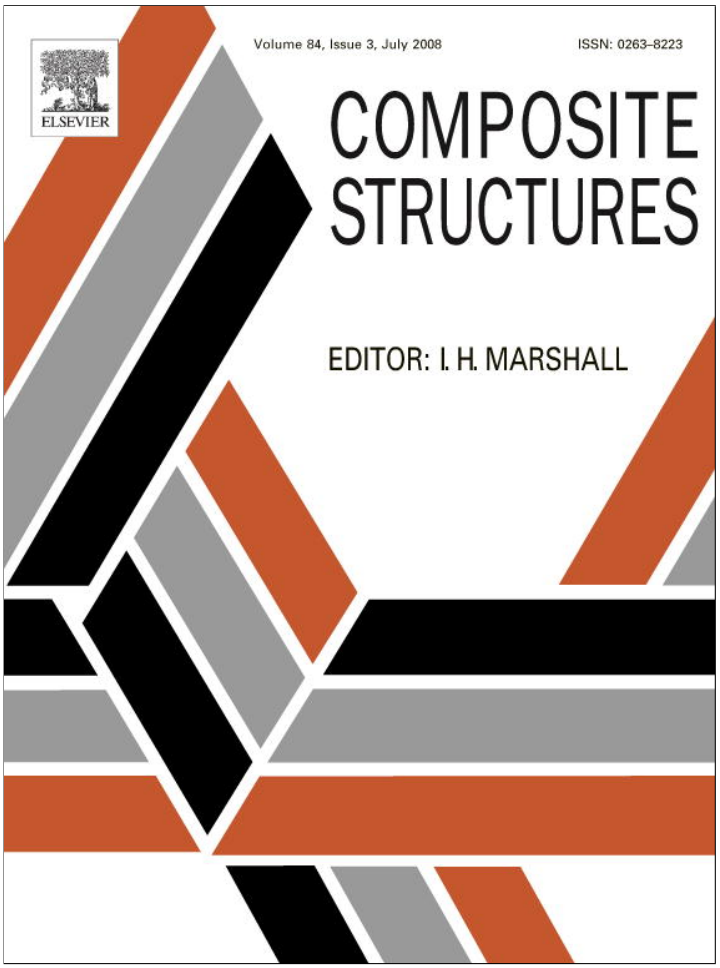

Available online at www.sciencedirect.com
ScienceDirect
Composite Structures 84 (2008) 199–208
COMPOSITE STRUCTURES
www.elsevier.com/locate/compstruct

Shock loading and drop weight impact response of glass reinforced polymer composites

Michael Hebert, Carl-Ernst Rousseau *, Arun Shukla

Department of Mechanical Engineering, University of Rhode Island, 222-B Wales Hall, Kingston, RI 02881, United States

Available online 27 July 2007

Abstract

Response of E-glass reinforced vinyl ester and urethane panels of varying structures subjected to shock loading and drop weight impact loading have been studied. Shock waves are created using a shock tube with a testing range of 3.08–7.53 MPa peak incident pressure. The materials performance under shock loading was evaluated by post-mortem visual damage assessment, residual compressive strength, and permanent deformation mapping of the panels. Drop weight impact performance was measured by energy absorbed by the samples, depth of penetration, and extent of internal damage. Glass preforms having total areal weights 144 and $216^{oz}/_{yd^2}$ (4.88 and $7.32^{kg}/_{m^2}$) were infused with either one of three separate types of vinyl ester and one urethane resin. The results show that urethane panels having total glass preform areal weight of $216^{oz}/_{yd^2}$ ($7.32^{kg}/_{m^2}$) performed better than similar vinyl ester resin panels. It was also found that of two materials with identical vinyl ester resins having total preform areal weight of $144^{oz}/_{yd^2}$ ($4.88^{kg}/_{m^2}$), the one with a finer glass structure consistently performed better in all evaluation criteria for shock wave and drop weight impact testing.

Keywords: Shock loading; Shock tube; Impact testing; Glass reinforced composites

1. Introduction

The response of composite materials subjected to dynamic loading has received much attention recently. Application of the materials can be found both in the transportation industry and in military structures. These materials are being used increasingly due to their superior strength, light weight, and adaptable design. However, in dynamic situations their behavior is very complex due to a large number of factors that govern the response. These factors include the strain rate sensitivity of many properties of the polymer resin [1], the arrangement of fibers, and thickness of the material [2]. Further developing the understanding of composite materials behavior under impulsive loading conditions is crucial for applications such as transportation of explosive material, collision, and use as armor. Common methods of dynamically loading composite materials are shock wave loading by use of explosives [3] and shock tubes [4–6], high velocity impact loading [7–9], and drop weight impact tests [2,10].

The use of shock tubes to create impulsive loading scenarios is preferred over the use of explosives given that shock tubes allow for the formation of a planar and uniform wave front [4]. Indeed uniformity in loading is crucial to both precise experimental measurements and modeling purposes. Measurements often taken from materials subjected to shock loading are plate deflection during loading [6], post-mortem compressive strength, permanent deformation, and visual assessment [5]. These allow for comparative analysis of various material structures. Other work has also been undertaken to develop numerical formulations for these materials when subjected to shock loading [4,11].

Impact loading behavior of glass fiber reinforced polymer composites has been studied primarily to evaluate stress wave progression in these materials [7–9]. Other studies have used drop weight impact testing to provide comparative results of the damage resistance of different

* Corresponding author. Tel.: +1 401 874 2542; fax: +1 401 874 2355.
E-mail address: rousseau@uri.edu (C.-E. Rousseau).

0263-8223/$ - see front matter © 2007 Elsevier Ltd. All rights reserved.
doi:10.1016/j.compstruct.2007.07.002

material types [2,10]. These studies measure force, acceleration, velocity, displacement, and energy during the impact event and focus mainly on the energy absorbed by the samples and visible damage as evaluation criteria.

The present study focuses on a series of woven E-glass reinforced polymer resin sheets (manufactured by VectorPly, Rhode Island) subjected to both shock wave loading and drop weight impact loading. These panels display variations in the polymer resin material and in the areal weight of the fiber preforms. Post-shock loading measurements include visual damage assessment, residual compressive strength, and plots of permanent deformation. Drop weight impact test measurements include total energy absorbed, depth of penetration, and extent of radial internal damage. The assessment method is primarily comparative and judges material performance as a function of resin type and internal structure.

2. Materials

A series of E-Glass reinforced polymer panels was manufactured by VectorPly. Each type of panel was constructed from one of three different glass preforms having areal weights of $36^{oz}/_{yd^2}$ $(1.22^{kg}/_{m^2})$, $72^{oz}/_{yd^2}$ $(2.44^{kg}/_{m^2})$, or $108^{oz}/_{yd^2}$ $(3.66^{kg}/_{m^2})$, and either a vinyl ester or a urethane resin. The $36^{oz}/_{yd^2}$ $(1.22^{kg}/_{m^2})$ preforms (E-2LTi 3600) consist of four plies of areal weights $9^{oz}/_{yd^2}$ $(0.31^{kg}/_{m^2})$ with layered orientation alternating between 0° and 90° as seen in Fig. 1. The dry preforms are stitched together in order to hold position and structure with a polyester fiber as seen in Fig. 2. The stitching is performed carefully, such as to avoid crimping, which can become a source of stress concentration. The $72^{oz}/_{yd^2}$ $(2.44^{kg}/_{m^2})$ preforms (E-2LTi 7200) consist of four plies of areal weights $18^{oz}/_{yd^2}$ $(0.61^{kg}/_{m^2})$ layered in the same manner as the 3600 preform. Separate vinyl ester resin panels were made of two $72^{oz}/_{yd^2}$ $(2.44^{kg}/_{m^2})$ and four $36^{oz}/_{yd^2}$ $(1.22^{kg}/_{m^2})$ preforms so that the thickness and total areal weight of glass were the same. Hence the materials vary only in relation to the structure of the glass. The $108^{oz}/_{yd^2}$ $(3.66^{kg}/_{m^2})$ preforms (E-3LTi 10800) consist of six plies of areal weights $18^{oz}/_{yd^2}$ $(0.61^{kg}/_{m^2})$ with layered orientation alternating between 0 ° and 90 °. All glass preforms have tensile and compressive strengths of 438 MPa and elastic modulus of 23 GPa in both the warp (0 °) and fill (90 °) directions.

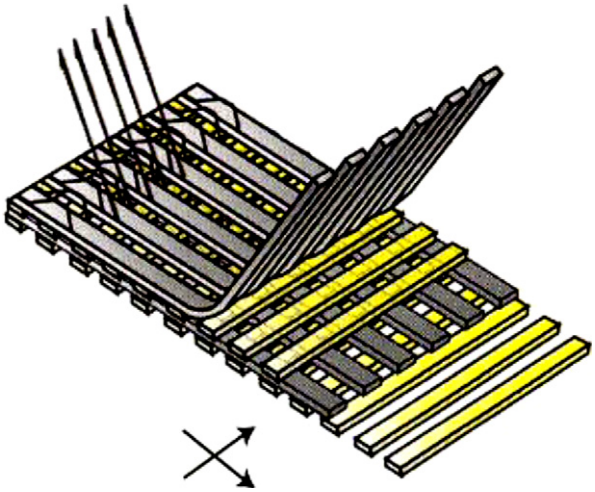

Fig. 1. $36^{oz}/_{yd^2}$ $(1.22^{kg}/_{m^2})$ E-glass preform diagram (E-2Lti 3600).

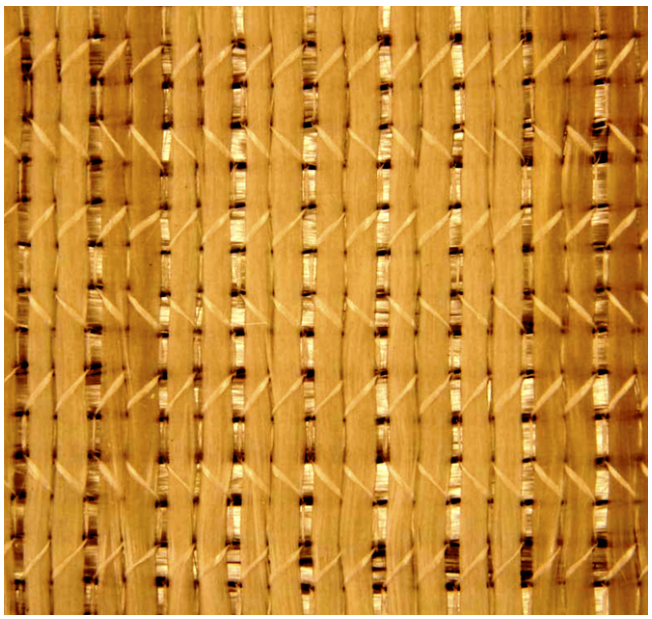

Fig. 2. $36^{oz}/_{yd^2}$ $(1.22^{kg}/_{m^2})$ E-glass preform prior to polymer infusion.

The polymer is added to the preforms in a close molded infusion process. The non-crimped and spaced perform layout allows for proper flow of polymer throughout the panel. Panels having total areal weights of $144^{oz}/_{yd^2}$ $(4.88^{kg}/_{m^2})$ have final laminate thickness between 4.3 mm and 4.8 mm, while the panels of weights $216^{oz}/_{yd^2}$ $(7.32^{kg}/_{m^2})$ are 5.6–6.2 mm thick. The variation in thickness is due to pressure from the vacuum bag during the manufacturing process. Table 1 lists the six types of composite materials that were studied.

3. Methods of evaluation

3.1. Dynamic evaluation of pure resins

To further supplement the mechanical characteristics of the pure resins, high strain rate compression tests were performed using a split-Hopkinson pressure bar (SHPB). Thin, cylindrical specimens are located between incident and transmitted aluminum bars, both of which are prepared with strain gages located at equal distance from the specimen. A third bar, the striker bar is fired into the incident bar to create a strain pulse. As the pulse reaches the specimen, part of the pulse is reflected due to the material mismatch, and part is transmitted through the specimen and into the transmitter bar. Using the recorded strain waves and one-dimensional wave propagation theory, the following equations are derived to determine the stress and strain history in the specimen [12,13] :

Table 1
Panels and compositions

Panel type	Resin	Resin tensile modulus (GPa)	Resin tensile strength (MPa)	Glass structure	Fiber content per preform ($^{oz}/_{yd^2}$)/($^{kg}/_{m^2}$)	# of Preforms
2 × 108 Urethane	RS technologies version	2.4	88.5	E−3LTi 10800	108/3.66	2
2 × 72 Urethane	RS technologies version	2.4	88.5	E−2LTi 7200	72/2.44	2
2 × 108 Vinyl ester (1)	Ashland Derakane 411–350	3.2	86.0	E−3LTi 10800	108/3.66	2
2 × 108 Vinyl ester (2)	Reichhold Hydrex 100HF	3.8	83.4	E−3LTi 10800	108/3.66	2
2 × 72 Vinyl ester	Hexion 781–2140	3.4	82.7	E−2LTi 7200	72/2.44	2
4 × 36 Vinyl ester	Hexion 781–2140	3.4	82.7	E−2LTi 3600	36/1.22	4

$$\sigma(t) = E\left(\frac{A}{A_s}\right)\varepsilon_T, \tag{1}$$

$$\varepsilon(t) = \frac{-2C_0}{L}\int \varepsilon_R \, dt, \tag{2}$$

where A_s is the specimen cross sectional area, ε_T is the transmitted strain, ε_R is the reflected strain, C_0 is the wave speed in aluminum, and L is the specimen thickness. Specimens of thickness 3.175 mm (0.125 in.) and diameter 9.525 mm (0.375 in.) were cut from the pure resin samples and tested using a 13 mm (0.5 in.) diameter SHPB testing apparatus. Strain data was recorded using dynamic strain recording instruments and processed using a MATLAB code to obtain dynamic stress–strain curves.

3.2. Drop weight impact testing

Drop weight impact tests were performed on 10.16 cm by 10.16 cm (4 in. by 4 in.) plates, and the impact toughness calculated. The tests were performed on an Instron Dynatup model 9210 in. accordance to ASTM D7136 [14]. The clamping fixture presented in Fig. 3 was used to secure the sample and prevent rebound. A 12 kg mass was dropped from a height of 46.6 cm such as to provide at least 3 m/s of impact velocity and 55 J of total impact energy. The data was recorded from a dynamic load cell located in the tup head and from a velocity flag positioned to monitor tup velocity during the impact process.

From the recorded load, time, and initial velocity the following integration yields the tup velocity versus time curve

$$v(t) = v_o - \int \frac{F(t)}{m}\, dt, \tag{3}$$

where v_o is the initial velocity measured by the flag at impact. The displacement of the impactor over time is found by

$$\delta(t) = \int v(t) dt. \tag{4}$$

Integrating the load versus deflection yields an energy absorbed over time curve:

$$E(t) = \int F(t)\frac{d\delta(t)}{dt}\, dt. \tag{5}$$

The total energy absorbed by the samples is used as a measure of materials toughness. Post-mortem measurements include the depth of the indentation and damaged area. Indentation depth was calculated according to the ASTM standard using a depth micrometer and two gage blocks positioned 2.5 cm from the impact site. The extent of the visual internal damage was measured radially from the center of the indentation at eight locations as shown in Fig. 4 to estimate an average damage radius and area.

3.3. Shock tube testing

A shock tube was used to generate high pressure, short duration shock waves with planar wave fronts. Fundamentally, a shock tube is a long cylinder divided into a high pressure (driver) section and low pressure (driven) section by a diaphragm. A sufficient pressure difference causes the diaphragm to burst, generating a subsequent rapid expansion of gas. Conservation of mass, energy, and momentum has been used to generate the following relationships for the pressure, temperature, and density in front of and behind this shock wave [15]:

$$\frac{P_2}{P_1} = \frac{2\gamma M_1^2 - (\gamma - 1)}{\gamma + 1}, \tag{6}$$

$$\frac{T_2}{T_1} = \frac{[2\gamma M_1^2 - (\gamma - 1)][(\gamma - 1)M_1^2 + 2]}{(\gamma + 1)^2 M_1^2}, \tag{7}$$

$$\frac{\rho_2}{\rho_1} = \frac{M_1^2(\gamma + 1)}{(\gamma - 1)M_1^2 + 2}, \tag{8}$$

where γ is the ratio (C_p/C_v) of specific heats of the driver gas, M_1 is the mach number of the shock wave relative to the driven gas, and subscripts 1 and 2 represent properties ahead of and behind the shock wave front, respectively. Eqs. (6)–(8) are valid for the following assumptions of the gas flow: one-dimensional flow, the gas is ideal and has constant specific heats, heat transfer

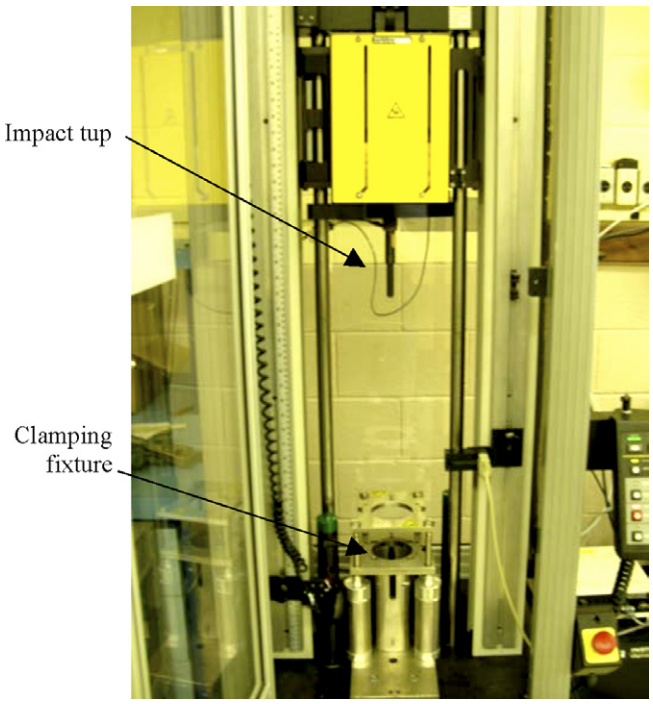

Fig. 3. Dynatup 9210 used for drop weight impact experiments.

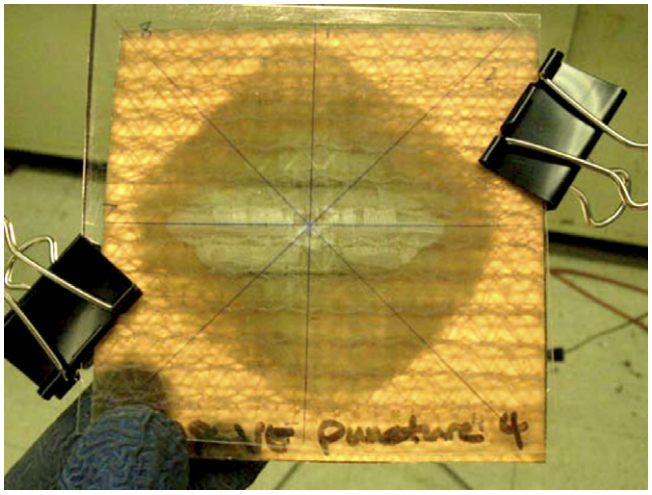

Fig. 4. Internal damage of drop weight impact sample.

and viscosity effects are neglected, and diaphragm rupture is instantaneous and does not disturb the subsequent gas flow.

The aforementioned shock tube has a total length of 7.92 m (26 ft) and consists of a 1.83 m (6 ft) long driver section with an inner diameter of 15.24 cm (6 in.), and a 6.10 m (20 ft) long driven section of inner diameter of 15.24 cm that tapers to 7.62 cm (3 in.). The driver section is pressurized using Helium until the barrier is ruptured releasing a shock wave through the driven section towards the tested plate. Mylar sheets with thickness of 0.254 mm (0.01 in.) were chosen as barriers for their strength and ability to rupture at a consistent pressure. Additional Mylar sheets were layered in the diaphragm to increase the burst pressure.

The burst pressure at which the Mylar ruptured was recorded using a pressure sensor (PCB 1501B02EZ5KP-SIG) adjoined to an oscilloscope. The shock wave pressure was recorded using a separate pressure sensor (PCB 134A23), located within the tube wall, 18.415 cm (7.25 in.) from the opening of the tube. The signal was sent through a signal conditioner (PCB 482A22) before being recorded by the Tektronix TDS 3014B oscilloscope.

Material samples of size 30.48 cm by 30.48 cm (12 in. by 12 in.) were fully clamped around the boundaries leaving a 22.86 cm by 22.86 cm (9 in. by 9 in.) area to be subjected to the loading. A schematic of the clamping fixture is presented in Fig. 5. The fixture is attached to a sturdy dump tank to contain the blast. Slippage at the boundaries was prevented by eight large c-clamps placed around the fixture and aluminum oxide 80 grit sandpaper bonded around the edges of the panels.

When the shock wave reaches the sample at the end of the tube, the wave is reflected into the shock tube. The reflected shock wave raises the temperature and pressure of the already shocked region, resulting in an increase in the shock pressure profile taken from the tube wall [16]. To understand the pressure profile to which the panel is subjected, a thick steel plate with a pressure sensor mounted at its center was clamped in the fixture. The burst, shock, and peak incident pressures were recorded for various numbers of Mylar barriers previous to experimentation. To calibrate the shock tube, the results were fit using a power law, and plotted as presented in Fig. 6.

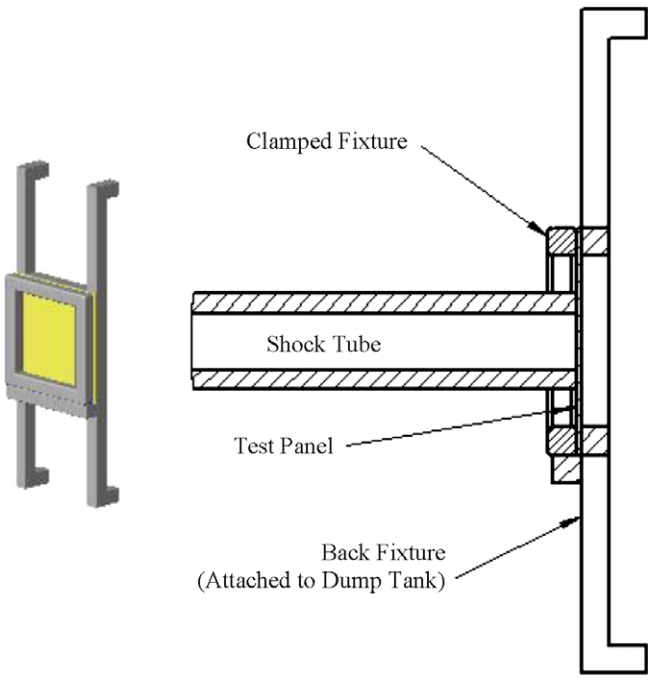

Fig. 5. Shock tube fixture.

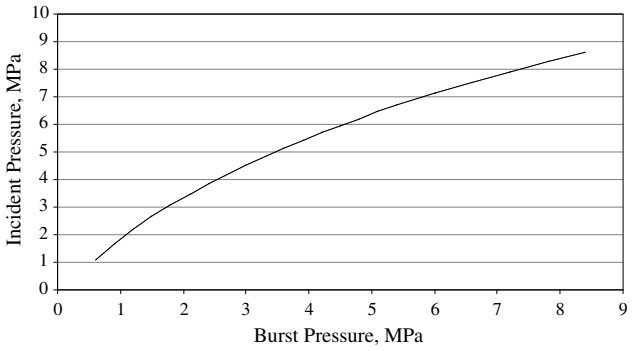

Fig. 6. Incident pressure (which panels are subjected to) vs. barrier burst pressure.

3.4. Post-mortem compression testing

To quantify the materials performance under shock loading conditions, five coupons were cut from the center of each panel and subjected to a quasi-static compressive testing. ASTM D3410 [17], a standard test method for determining compressive properties of cross-ply fiber–resin composites, was followed. The tests were performed on an Instron 5582 testing machine using specimens of length 152.4 mm (6 in.), width 19.05 mm (0.75 in.) and a gage length of 12.7 mm (0.5 in.). The load was transferred through shear upon the gripped areas, using the fixture described in previous research [5], where post-mortem compressive strength was determined on similar panels. Aluminum oxide 80 grit sandpaper was bonded to the gripped area of the coupons to prevent slippage. A schematic showing the location of the coupons is shown in Fig. 7. All testing was performed in the warp direction for uniformity in the comparative evaluation. When the coupons were unable to support further load, the maximum load was recorded, and the compressive strength of the sample was calculated. The average of the five coupons was used as the panel's compressive strength.

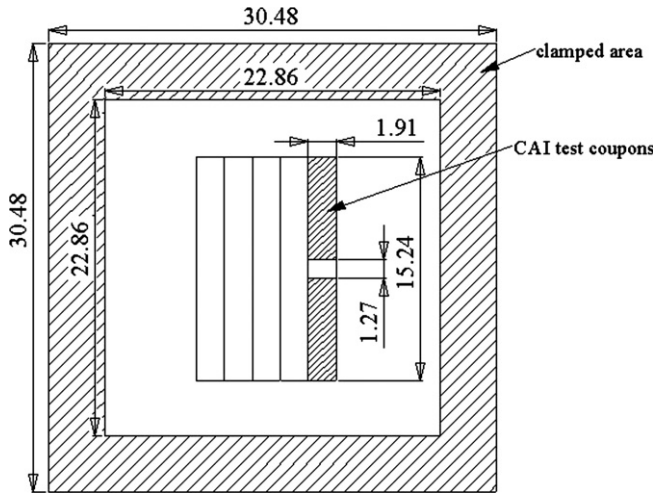

Fig. 7. Layout of panels subjected to shock tube loading.

3.5. Evaluation of permanent deformation

At high incident shock tube pressures (>5.72 MPa), some panels were found to maintain a large amount of permanent deformation. This deformation was mapped by placing the panels on a table with a movable *x-y* axis controlled by stepper motors. The table was connected to a computer and programmed to move in 10 mm (0.4 in.) steps. A laser capable of recording distances in the range of 10–40 mm was mounted above the panel. The laser signal was sent to the computer and was recorded between steps. The laser obtained the best signal reading black surfaces, therefore the panels were duct taped and spray-painted flat black. A Matlab computer code was used to process and plot the recorded data.

4. Experimental results

4.1. SHPB testing of pure resins

The dynamic stress–strain behavior of the pure resins is presented in Fig. 8. The SHPB technique is not ideal for obtaining values of dynamic modulus or yield stress, as the material is not in a stress equilibrium state during deformation [13]. Thus, it is only noted that dynamically the urethane shows noticeably stiffer behavior, though statically it was found that all the vinyl ester resins have a stiffer modulus as seen in Table 1.

4.2. Drop weight impact of virgin materials

Drop weight impact tests were performed and load, velocity, displacement, and energy history were retrieved during the event. Representative plots of resulting load, velocity, and displacement versus time are shown in Fig. 9a–c. These curves are used to generate the following. First, the load is plotted against the displacement, as shown in Fig. 9d. The resulting figure is then integrated to obtain the energy versus time curve as shown in Fig. 9e. It is seen that at a critical time circa 5.5 ms, the displacement reaches a maximum as velocity reaches zero. At this time, all the

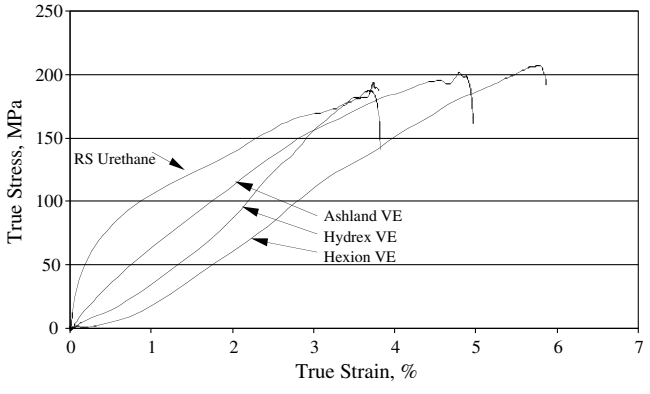

Fig. 8. Stress–strain response of resins obtained from SHPB tests, $\dot{\varepsilon} = 1.7 \times 10^3$.

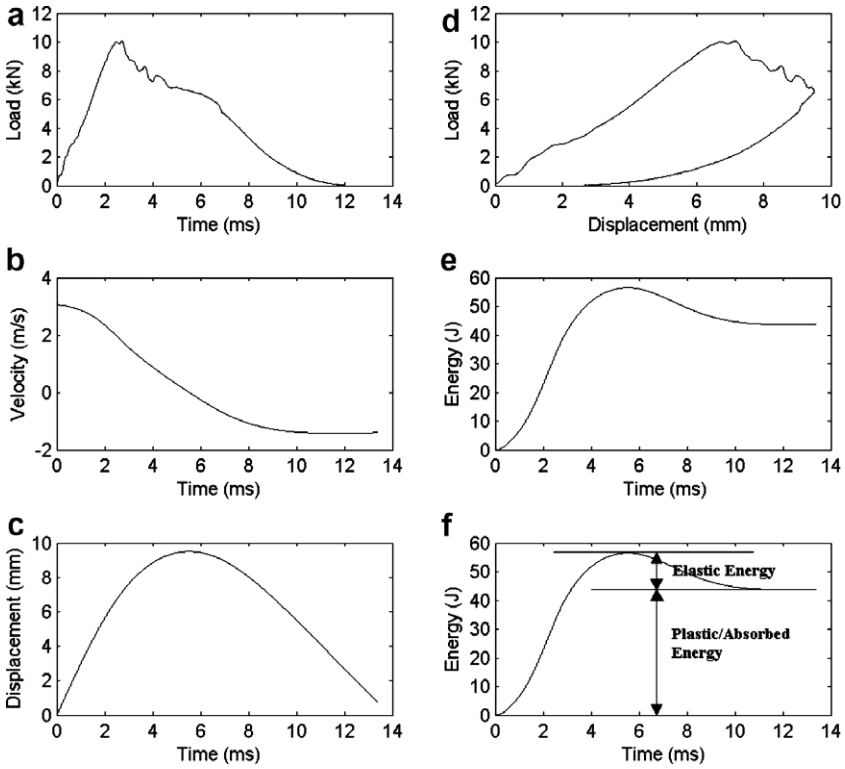

Fig. 9. Drop weight impact experiment plots.

energy has been transferred from the tup into the specimen. The energy is stored as both elastic energy and plastic energy. The latter includes deformation and damage components. The decrease in the energy absorbed following the critical time can be attributed to the stored elastic energy causing the tup weight to rebound. The remaining energy absorbed in the material is damage and plastic energy, and is representative of the level of damage suffered by the sample, as indicated in Fig. 9f. A lower final energy absorbed would therefore, correspond to a material more resistant to impact, so long as the sample absorbs all the energy from the tup and causes the weight to rebound. Evaluation of the energy absorbed was further verified by monitoring of velocity profiles throughout the test. The derived change in kinetic energy correlated faithfully with the absorbed energy evaluated above, thus provides an alternative methodology for implementing and energy criterion. Table 2 presents the total energy absorbed by the material, the depth of penetration by the tup head, and the extent of visible internal damage. Two samples of each material were tested to verify consistency, and the results were averaged.

The data is normalized with respect to the sample thickness. The 2×108 urethane resin samples show superior impact resistance as measured by energy absorbed, depth of penetration, and damaged area compared to all other materials. On the other hand, the 2×72 urethane was the weakest material as measured by energy absorbed and penetration, though little damage is observed radially in these samples. It should be noted that, generally the two different

Table 2
Drop weight impact test results

Material	Thickness (mm)	Energy absorbed per unit thickness (J/mm)	Depth of indentation per unit thickness (mm/mm)	Estimated damaged area per unit thickness (cm̂2/mm)
(2×108) Vinyl ester(1)	5.59	6.59	0.21	2.18
(2×108) Vinyl ester(2)	5.59	5.46	0.21	8.56
(2×72) Vinyl ester	4.70	9.10	0.77	2.02
(4×36) Vinyl ester	4.45	8.75	0.63	1.86
(2×108) Urethane	6.35	4.54	0.14	1.25
(2×72) Urethane	3.94	10.19	0.88	1.23

2×108 vinyl ester resin samples displayed similar impact resistance. However vinyl ester(2) sustained greater visible internal damage than vinyl ester(1). The 4×36 structured vinyl ester samples appears to be slightly superior to the 2×72 samples of the same resin based on all evaluation criteria.

4.3. Shock tube experiments

The plates were subjected to shock waves of peak incident pressures 3.08, 4.54, 5.72, and either 7.12 or

7.53 MPa. Damage was first observed in the form of fiber breakage around the boundaries and slight discolorations on the back surface of the plate. As shock pressures increased, the primary form of damage consisted of internal delamination spreading inwards from the boundaries. The amount of internal delamination is easily seen when the panels are placed over a bright light source. Figs. 10 shows the progression of damage in each type of panel. No images are available for the 2×108 vinyl ester(1) samples made from the Ashland resin.

The 2×108 urethane samples experienced little visible damage even at high incident pressures, as seen in Fig. 10(b). A similar damage progression was observed with 2×108 vinyl ester(1) panels. On the other hand, the 2×108 vinyl ester(2) suffered from significant delamination beginning at low incident pressures (see Fig. 10(e)). These trends parallel those observed in the drop weight impact tests, where relatively extensive radial damage was found in the 2×108 vinyl ester(2) specimens. Figs. 10a,c,d show that all panels having total areal weights of $144^{oz}/_{yd^2}$ ($4.88^{kg}/_{m}^{2}$), both urethane and vinyl ester resin based, experienced damage progression comparable to each other.

The residual structural integrity of the panels was found by performing quasi-static compression tests on coupons

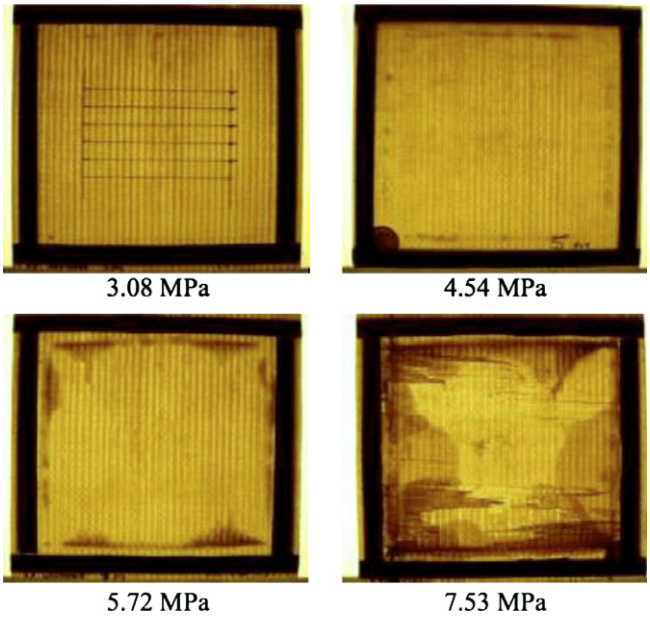

Fig. 10(a). Delamination of panels – 2×72 urethane.

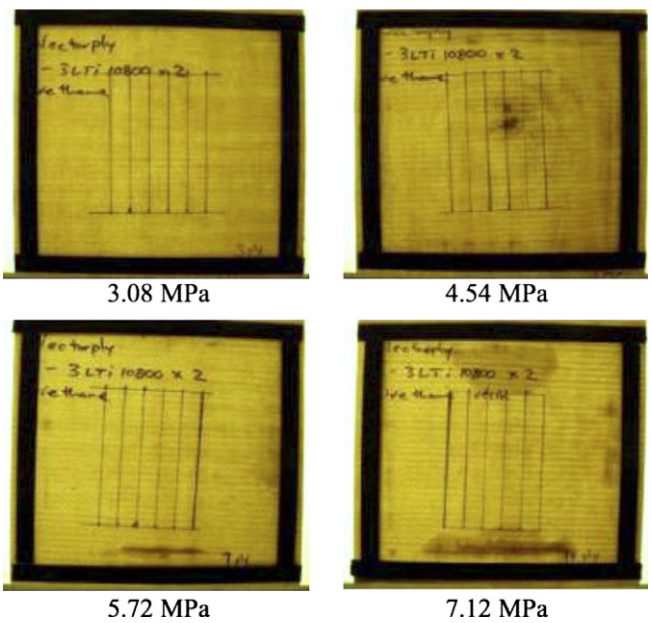

Fig. 10(b). Delamination of panels – 2×108 urethane.

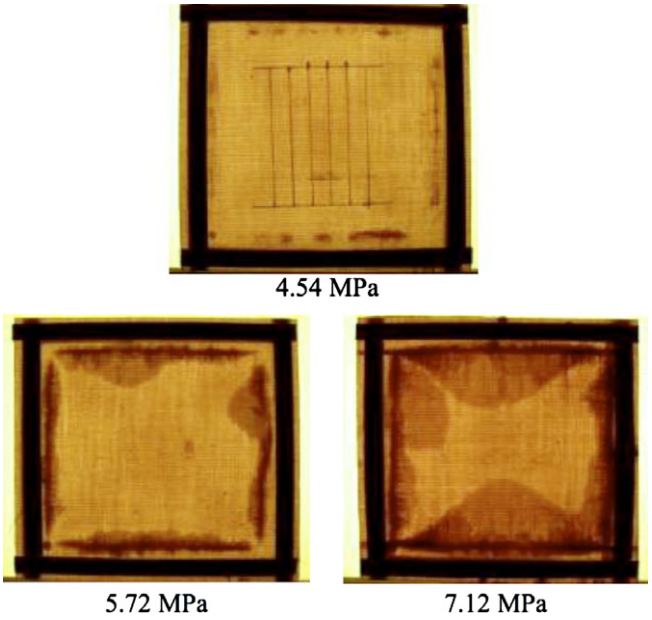

Fig. 10(c). Delamination of panels – 4×36 vinyl ester.

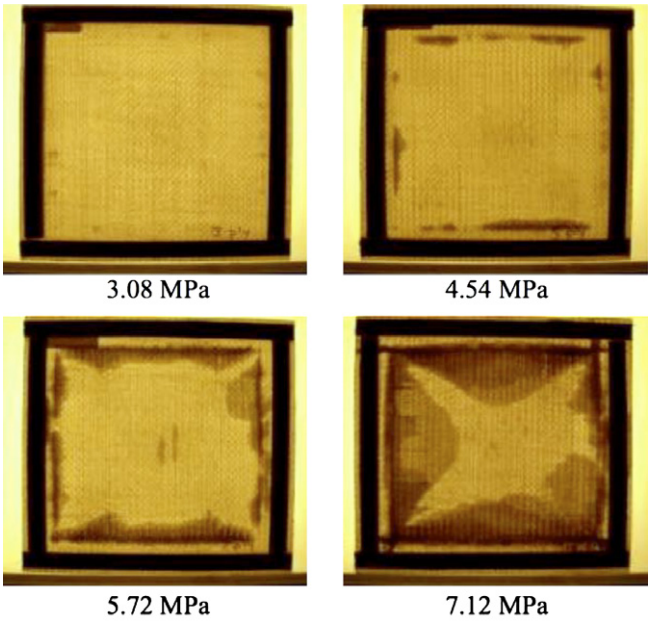

Fig. 10(d). Delamination of panels – 2×72 vinyl ester.

from the center of the panel. These tests were performed only on panels with low levels of permanent deformation, exhibiting no delamination at the center of the panel. Residual strengths were normalized by the strength of the virgin material and plotted as a function of incident pressure in Fig. 11.

As seen in the figure, all vinyl ester resin materials displayed similar behavior of increasing loss of strength with increasing pressure, with this increase becoming much more pronounced at higher pressures. Unexpectedly, the urethane resin materials showed a different trend where, following an initial decrease in strength with increasing pressure, the material then appears to recover some of this loss in strength as even higher pressure loading is imparted. This behavior has also been observed in shock loading of 3D weave composite panels [5]. In the present case, the surprising phenomenon may be due to the complex rate-sensitive behavior of urethane. It was found that at higher rates, the urethane becomes quite stiff relative to its static state. It is also known that at higher rates, polymers develop an out of phase lag between the stress and strain waves [18]. The portion of the stress–strain relation that is out of phase is known as the loss modulus. The ratio of loss modulus to the in phase modulus is known as the loss tangent. The loss tangent creates an energy damping effect on waves over a certain range of rates and could be inferred as the cause for the improved performance of urethane panels at higher rates.

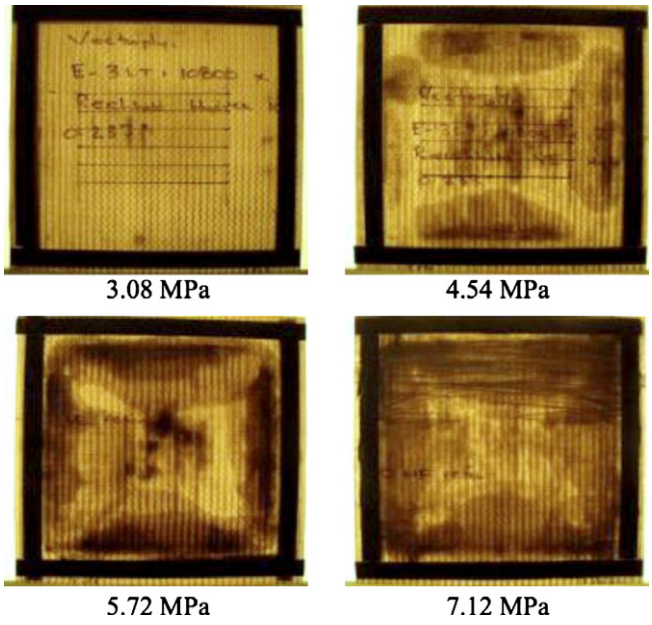

Fig. 10(e). Delamination of panels – 2×108 vinyl ester (2).

The 2×108 urethane and 2×108 vinyl ester(1) samples retained the most strength at highest incident shock pressures tested. Conversely, the 2×108 vinyl ester(2) material experienced the most dramatic loss of strength overall. At incident shock pressure of 5.72 MPa, internal delamination had spread far enough to disallow compression testing. This is evidently related to the rapid spread of internal damage seen even at low pressures and in impact tests.

It was found that the 4×36 and 2×72 vinyl ester materials experienced nearly identical loss of strength up to an incident pressure of 5.72 MPa. At this pressure, the strength of the 2×72 vinyl ester decreased to 60% of its initial value, while the 4×36 vinyl ester still retained 90% of its initial strength. The strength of the 2×72 urethane sample decreased to roughly 65% of its initial strength at a low incident pressure (3.08 MPa) – this was the most significant loss of strength of all panel types at this pressure. However, when tested at the higher pressure levels of 4.54 MPa and 5.72 MPa, the residual strength decreased to roughly 75%

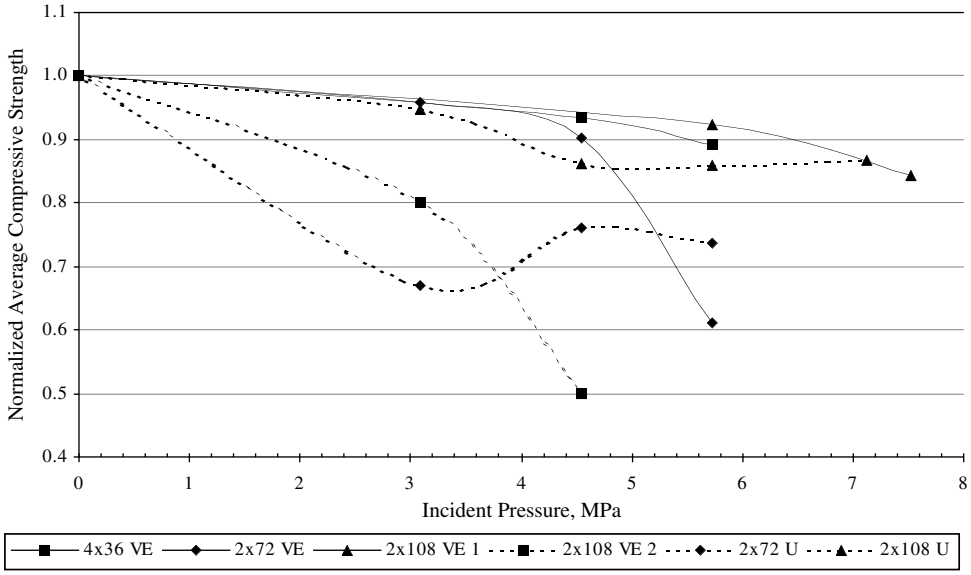

Fig. 11. Post-mortem compressive strength of panels vs. incident pressure.

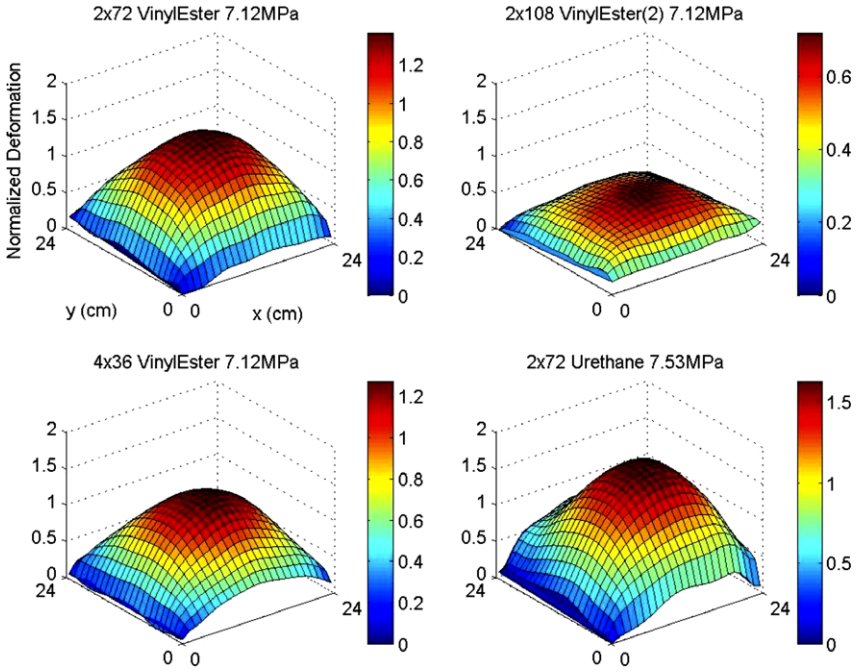

Fig. 12. Normalized deformation plots.

of its initial strength, thus resulting in better performance than the 2×72 vinyl ester samples at these higher pressures.

For panels with measurable amounts of permanent deformation, the profile was normalized with respect to the sample thickness and plotted as seen in Fig. 12. At high incident shock tube pressures (>7.12 MPa) the 2×72 urethane material suffered from the most significant permanent deformation. The 4×36 vinyl ester material experienced less significant deformation than the 2×72 vinyl ester. The 2×108 urethane and vinyl ester(1) samples had minimal permanent deformation even at these high pressures, thus are not presented in Fig. 12. The 2×108 vinyl ester(2) suffered from more significant deformation than the other 2×108 materials at this pressure, but still less than the lower areal weight materials. It should be noted that at 5.72 MPa this material sustained enough internal damage to disallow compression testing, while concurrently experiencing minimal deformation.

5. Conclusions

The 2×108 urethane material out-performed all materials in drop weight impact experiments and all materials, except the 2×108 vinyl ester(1) in the shock tube experiments. Although the 2×72 vinyl ester performed better than the 2×72 urethane in impact resistance and lower pressure shock resistance, the urethane material was found to be more resistant at higher incident shock pressures (>4.54 MPa). This improved behavior is not fully understood, but is believed to be due to the complex rate-sensitive behavior of the urethane matrix, as previously discussed. Should very high blast rates be anticipated, urethane matrix composites may offer a superior blast-resistant material alternative to vinyl ester matrix composites.

Two vinyl ester resin samples having fiber areal weight of 144 $^{oz}/_{yd^2}$ ($4.88^{kg}/_{m^2}$) were tested. The 4×36 pre-form structured material out-performed the 2×72 structured material in impact testing and shock loading experiments. This suggests that a finer structure of fibers may create a more blast-resistant composite than a coarser structure.

The responses of the two 2×108 vinyl ester resin materials varied greatly in both drop weight impact testing and shock tube experiments. Although the Hydrex and Ashland resin materials absorbed equal amounts of energy and were penetrated by the drop weight to equal depths, the Hydrex resin samples endured an extended spread of internal damage. This observation was reinforced when the samples were exposed to impulsive shock wave loading. Indeed, this damage spread triggered a drastic decrease in residual strength even at low shock pressures. As the vinyl ester resins share similar static properties, the varying results are likely to come from varying strain rate-sensitive properties of the resins or less efficient bonding mechanism of the Hydrex resin to the glass fibers.

Acknowledgement

This work was supported through funding from the University of Rhode Island Transportation Center (Grant Number 0000507), and the US Army (W911NF-04-1-0154). The authors thank Mr. Philip Steggall and Vector-Ply for providing materials for testing, Ashland, Hydrex, Hexion, and RS Technologies for supplying pure resin materials.

References

[1] Shah Khan MZ, Simpson G, Gellert EP. Resistance of glass-fibre reinforced polymer composites to increasing compressive strain rates and loading rates. Compos Part A 2000;31:57–67.

[2] Naik NK, Joglekar MN, Arya H, Borade SV, Ramakrishna KN. Impact and compression after impact characteristics of plain weave fabric composites: effect of plate thickness. Adv Comp Mater 2004;12:261–80.

[3] Mouritz AP. The effect of underwater explosion shock loading on the flexural properties of grp laminates. Int J Impact Eng 1996;18: 129–39.

[4] Stoffel M, Schmidt R, Weichert D. Shock wave-loaded plates. Int J Solids Struct 2001;38:7659–80.

[5] Leblanc J, Shukla A, Rousseau C, Bogdanovich A. Shock loading of three-dimensional woven composite materials. Compos Struct 2007;79:344–55.

[6] Stoffel M. A measurement technique for shock wave-loaded structures and its application. Exp Mech 2006;46:47–55.

[7] Zaretsky E, deBotton G, Perl M. The response of a glass fibers reinforced epoxy composite to an impact loading. Int J Solids Struct 2004;41:569–84.

[8] Dandekar DP, Hall CA, Chhabildas LC, Reinhart WD. Shock response of a glass-fiber-reinforced polymer composite. Compos Struct 2003;61:51–9.

[9] Boteler JM, Rajendran AM, Grove D. Shock wave profiles in polymer matrix composites. Shock Comp Cond Matter 1999. Presented at.

[10] Ku H, Cheng YM, Snook C, Baddeley D. Drop weight impact test fracture of vinyl ester composites: micrographs of pilot study. J Compos Mater 2005;39:1607–20.

[11] Dyka CT, Badaliance R. Damage in marine composites caused by shock loading. Compos Sci Tech 1998;58:1433–42.

[12] Gray III GT. Classic split-Hopkinson pressure bar testing. 10th ed. Metals Handbook, Mechanical Testing, vol. 8. ASM; 2000. p. 462–73.

[13] Lee OS, Kim MS. Dynamic material property characterization by using split Hopkinson pressure bar (SHPB) technique. Nucl Eng Des 2003;226:119–25.

[14] ASTM D 7136, Standard test method for measuring the damage resistance of a fiber-reinforced polymer matrix composite to a drop-weight impact event. ASTM International.

[15] Wright J. Shock Tubes. New York: John Wiley and Sons Inc.; 1961.

[16] Badiger SM. Design and fabrication of an experimental facility for controlled, transient shock wave loading. Masters Eng. Thesis, University of Rhode Island. 2004.

[17] ASTM D 3410, Standard test method for compressive properties of polymer matrix composite materials with unsupported gage section by shear loading. ASTM International.

[18] McCrum NG, Buckley CP, Bucknall CB. Principles of Polymer Engineering. 2nd ed. New York: Oxford Science Publications; 1997.